Evolution and WRF Uncertainties of an Amorphous Yet Intense Snow Band on 7 February 2020

Stony Brook University School of Marine and Atmospheric Sciences

UNIVERSITY of WASHINGTON

Phillip Yeh[1], Brian A. Colle[1], Joseph Finlon[2], Lynn A. McMurdie[2], Victoria McDonald[2], and Andrew DeLaFrance[2]

[1]School of Marine and Atmospheric Science, Stony Brook University, Stony Brook, NY

[2]Department of Atmospheric Sciences, University of Washington, Seattle, WA

1. Introduction

- Snowfall in NE US winter storms is often organized in bands that vary on spatial and temporal scales, from large primary snowbands to small-scale multibands
- A strong cyclone developed by 0000 UTC 7 February and tracked from southeast PA to southern ME as it deepened rapidly
- Intense snowfall (5-8 cm/h) in western and central NY after 1400 UTC, northwest of the low, but was not organized as a primary snowband
- Science questions addressed by this poster
  1. Why was there no primary band?
  2. What were the mechanisms for heavy snow during this event?
  3. How well does WRF simulate the event, and what is uncertainty in the model?

2. Data and Methods

- Three coordinated ER-2 (red) and P-3 (blue) West-East legs
- New York State mesonet precipitation totals
- WRFv4.0 (1-way nesting: 18-, 6-, and 2-km grid spacing)
  - 1800 UTC, 6 Feb initialization
    - **RAP ICs/BCs, P3 micro**
    - RAP ICs/BCs,Thompson
    - GFS ICs/BCs, P3 micro
    - ERA-5 ICs/BCs, P3 micro
  - 0000 UTC, 7 Feb initialization
    - RAP ICs/BCs, P3 micro
    - RAP ICs/BCs, Thompson micro

3. Radar Reflectivity Structure

- Broad region of >25 dBZ in NEXRAD (Fig. 1a)
- Does not meet primary band criteria in Novak et al. (2010)
  - Structure is transient and lasts <2h
  - Width of >30 dBZ region <20 km for the majority of the event
- Precipitation is more convective on eastern side, but not co-located with the amorphous band
- WRF captures the general region of enhanced reflectivity, but shifted slightly to the southwest (Fig. 1b)
- EXRAD captures a steady vertical layer of >30 dBZ above areas of heavy snow, lowering in altitude with time (Fig. 2)
- Ice mixing ratios >1.2 g/kg on west side (Fig. 3)

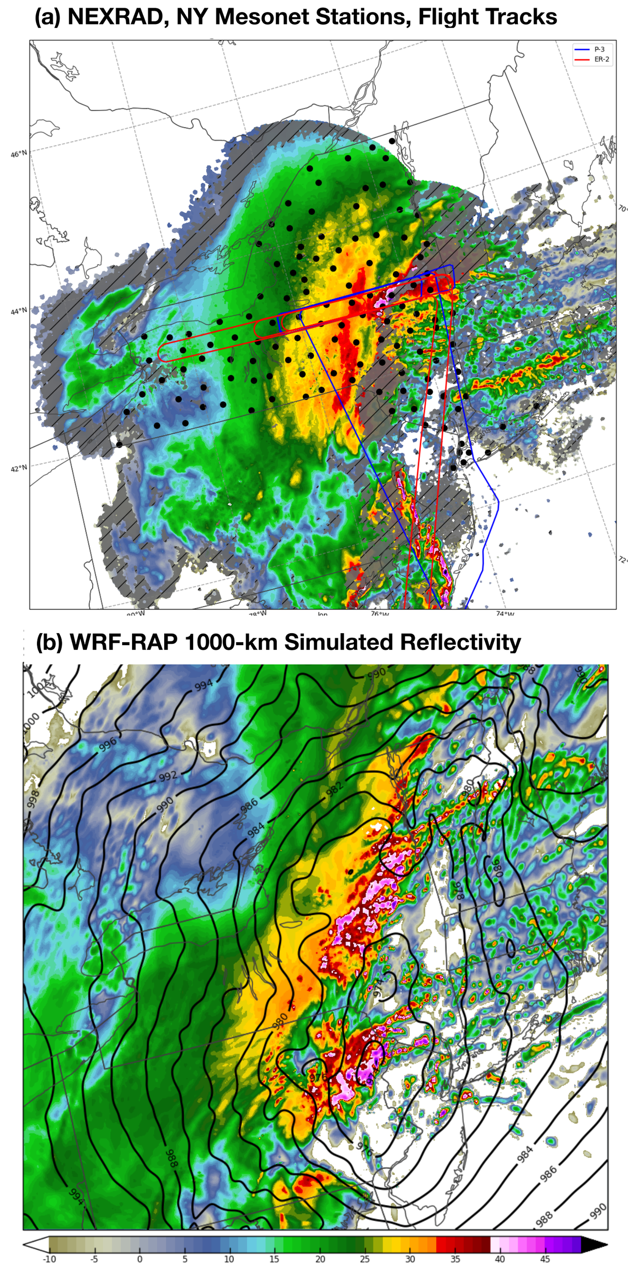

Fig. 1: Comparison of NEXRAD Reflectivity at 1529 UTC and WRF Simulated Reflectivity at 1530 UTC [dBZ]

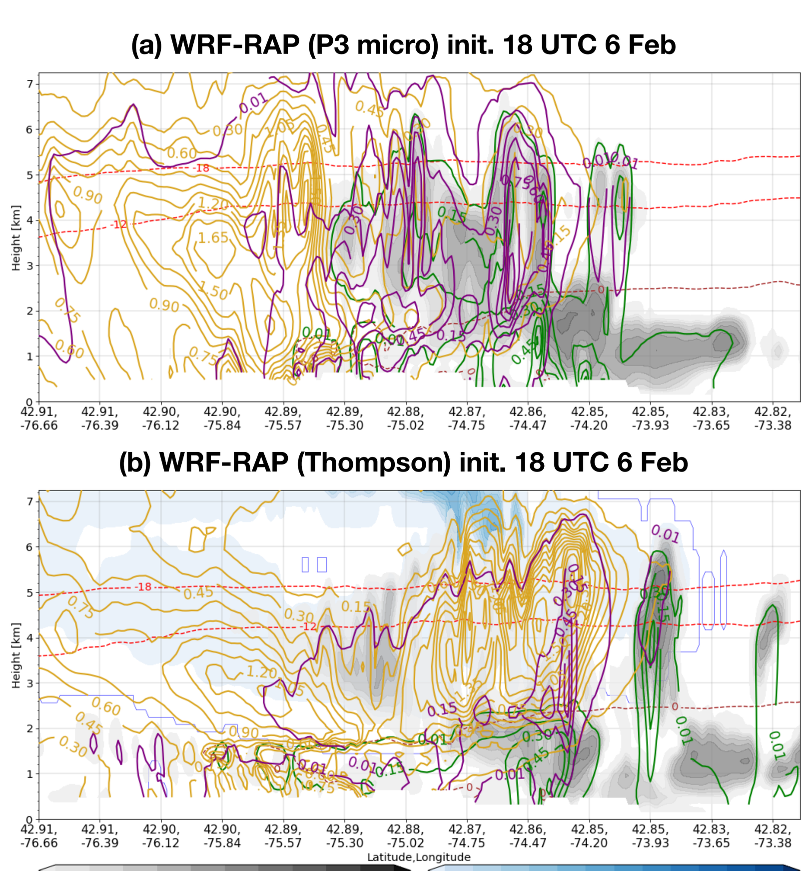

Fig. 3: WRF mixing ratios (g/kg), valid 1530 UTC 7 Feb; q_{dep}=gold, q_{rim}=purple, q_r=green, q_{cloud}=grays, q_{ci}=blues (10^6)

- P3 microphysics scheme produces significantly more rimed ice than Thompson scheme
- WRF suggests a deep layer of abundant supercooled water

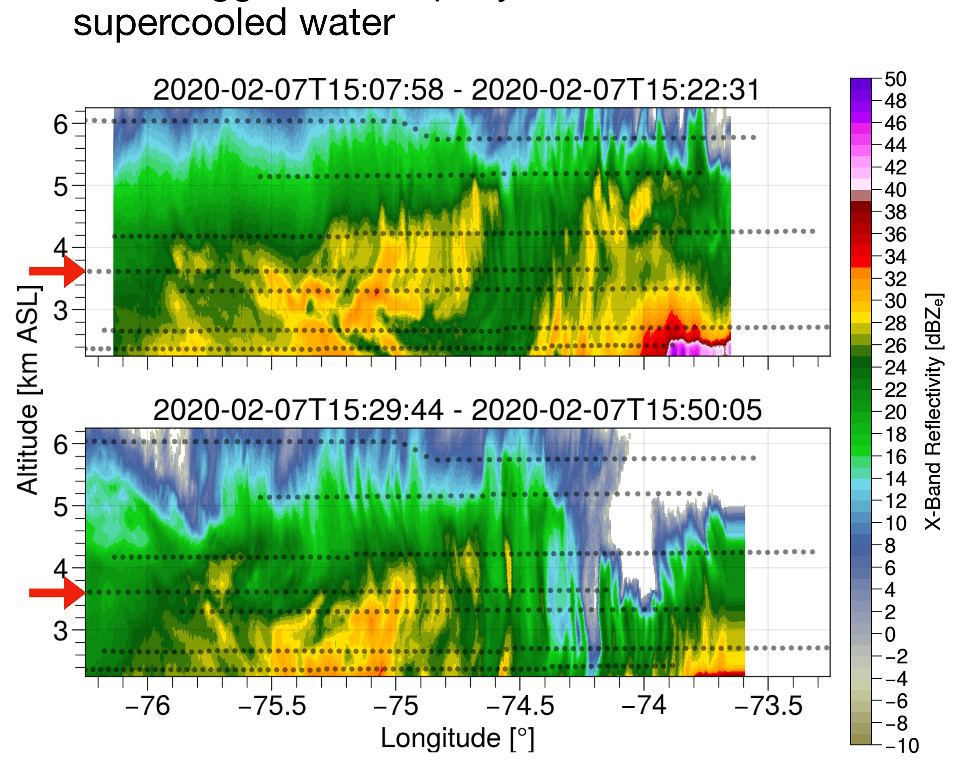

Fig. 2: ER-2 EXRAD Reflectivity (dBZ) with all P-3 tracks (dotted); red arrow marks the 1529-1550 UTC P-3 flight leg

3. Thermodynamic Structure

Fig. 4: RAP Analysis 700 hPa Heights, Temp at 16 UTC Feb. 7

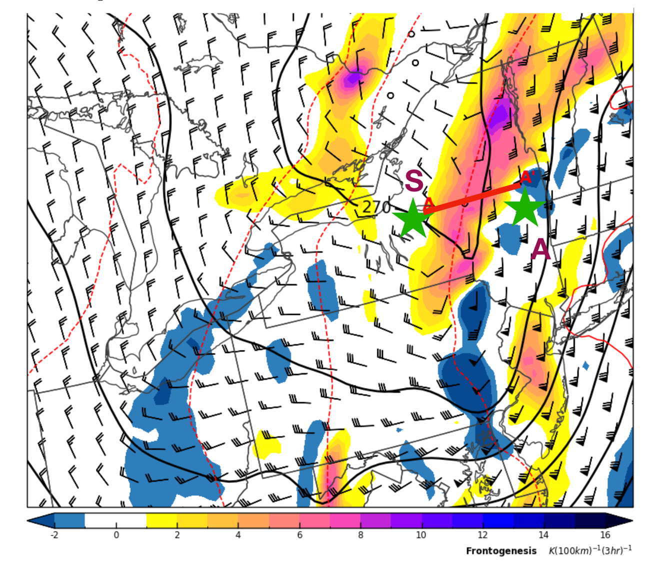

Fig. 5: Radiosonde (red, starred in Fig. 4) vs. WRF θ_e Profiles [K]

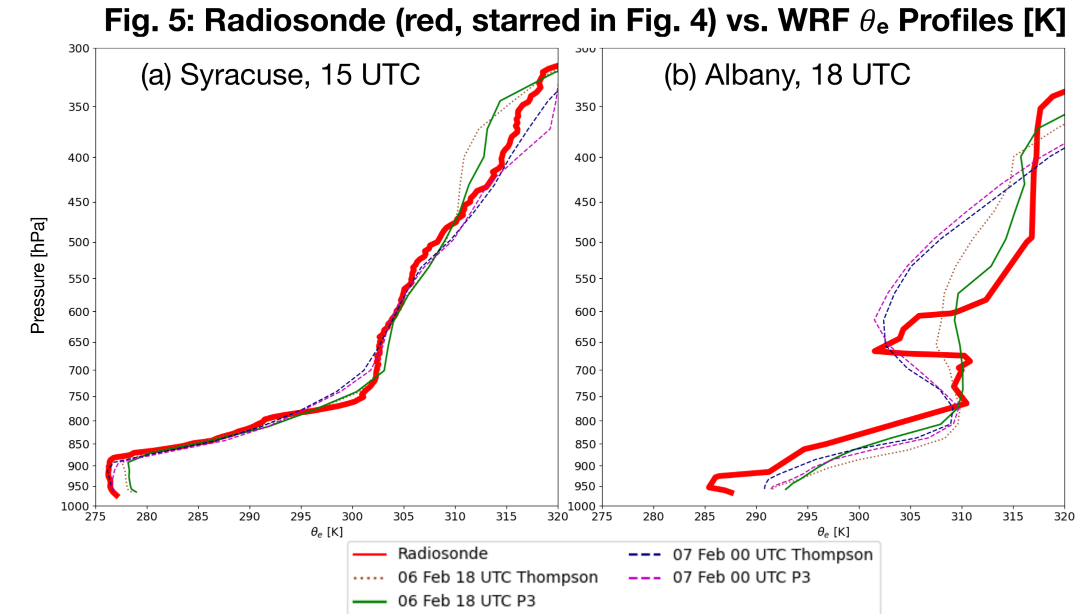

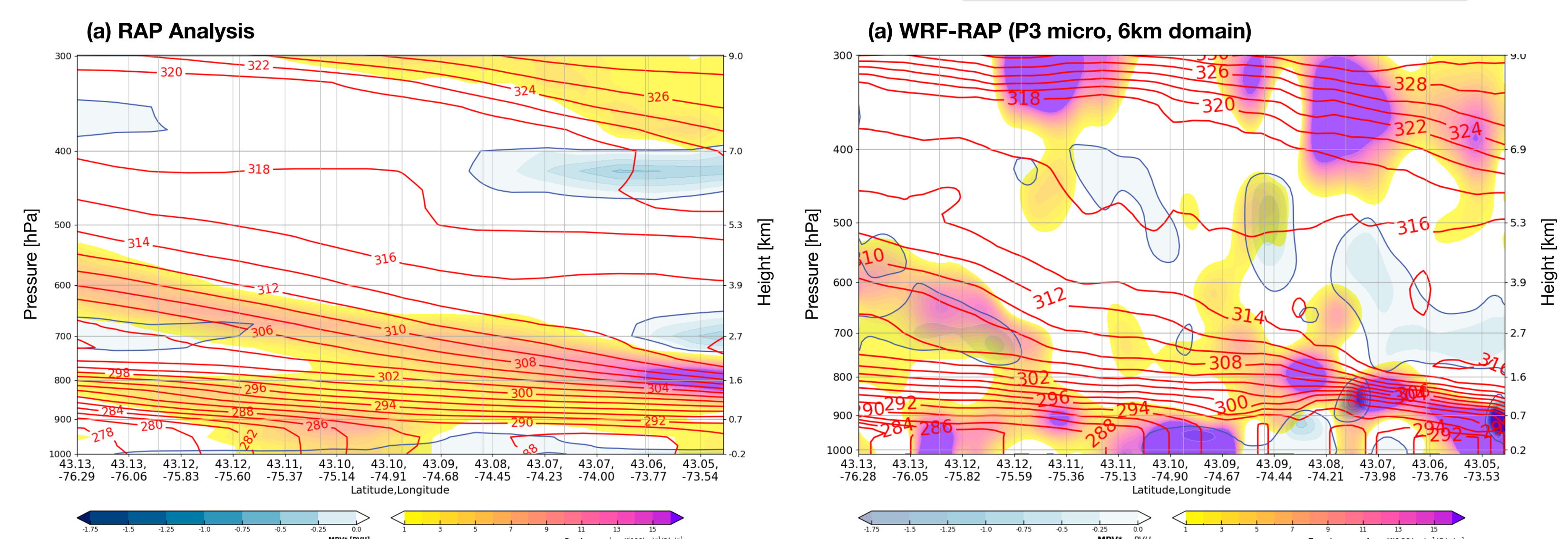

Fig. 6: Cross-Section θ_e* [K], Frontogenesis [K/100km/3h], –MPV* [blue: PVU] at 16 UTC Feb. 7

- Ill-defined 700 hPa low (Fig. 4)
- Potential stability decreases to the east in the soundings (Fig. 5)
  - Neutral 700~800 hPa layer in both locations
  - More stable above 700 hPa in Syracuse (5a) than in Albany (5b)
  - Models too warm at the surface
  - More model disagreement in Albany
- Frontogenesis >10 K/100km/3h throughout the event in RAP Analysis and WRF (Fig. 6)
  - Broad, sloping region (rather than concentrated) in the vertical
  - Elongated region co-located with the heaviest precipitation
  - WRF frontogenesis is more intense
- Region of –MPV* around 700 hPa, above the frontogenesis layer, decreasing to the east (Fig. 6)

4. Microphysics Evolution

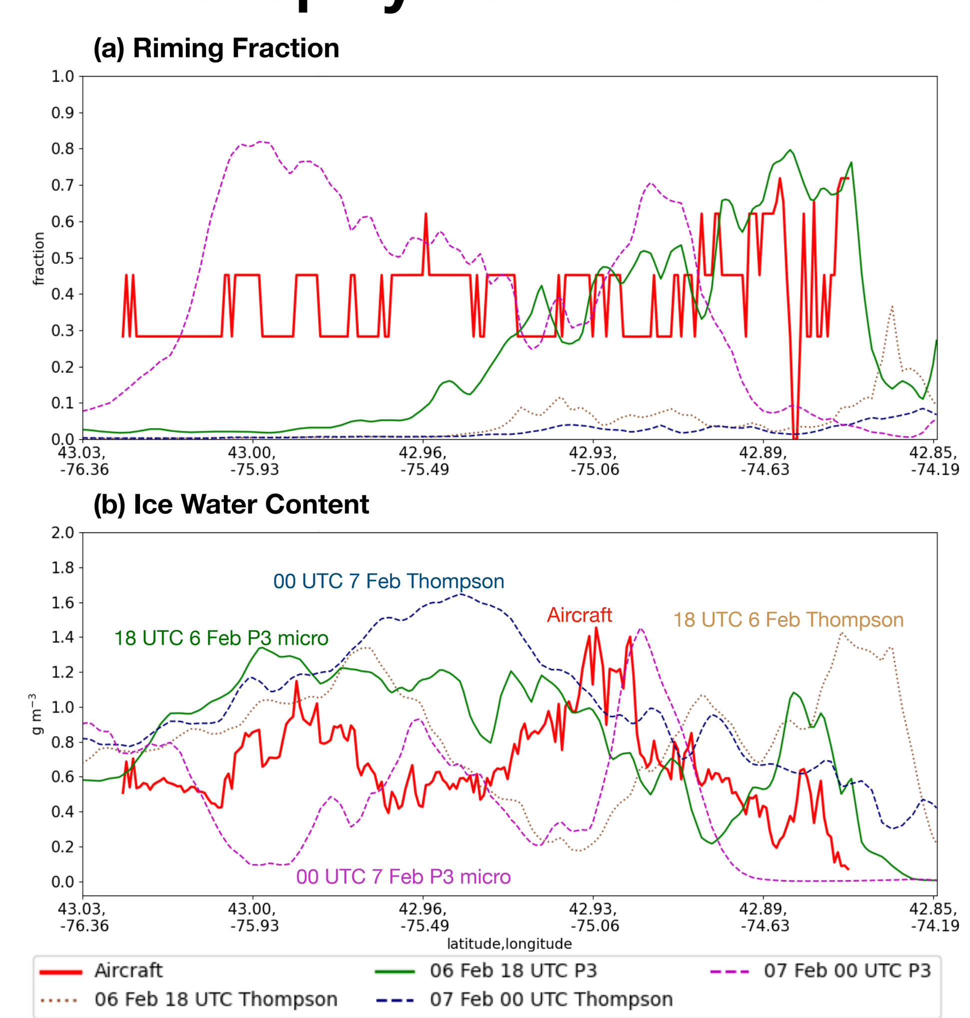

Fig. 7: Microphysics along 1529-1550 UTC P-3 flight leg (red arrow on Fig. 3), WRF valid 1530 UTC 7 Feb

- Aircraft microphysical variables derived from P-3 2DS/HVPS probes and ER-2 radar
- High degree of riming on the eastern half of the leg (Fig. 7a)
- Thompson scheme produces noticeably less riming
- GFS and ERA-5 initializations (also with P3 scheme) produce similar ranges of values to the RAP initializations with the P3 scheme (not shown)
- Models show the variability of IWC within the layer (Fig. 7b)
- High degree of riming observed with microphysics probes along the eastern half of the leg
- P-3 aircraft reports a high amount of aggregation in the 2 flight legs closest to the ground (<3 km altitude)

5. Surface Precipitation

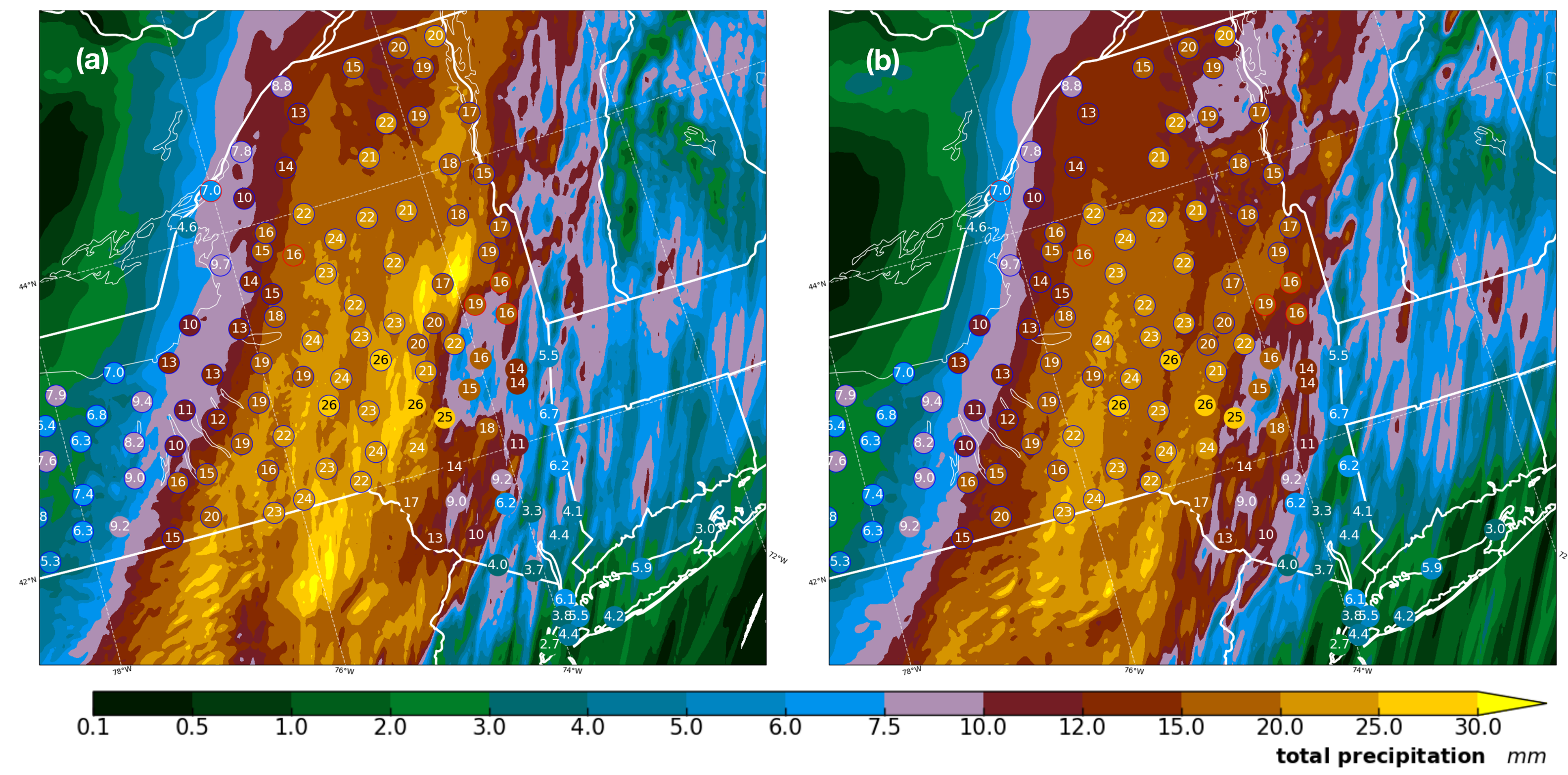

Fig. 8: 12-18 UTC Accumulated Precipitation [mm] for NY Mesonet (shaded circles with numbers) and WRF (shaded) for (a) 18 UTC P3 scheme and (b) 18 UTC Thompson scheme

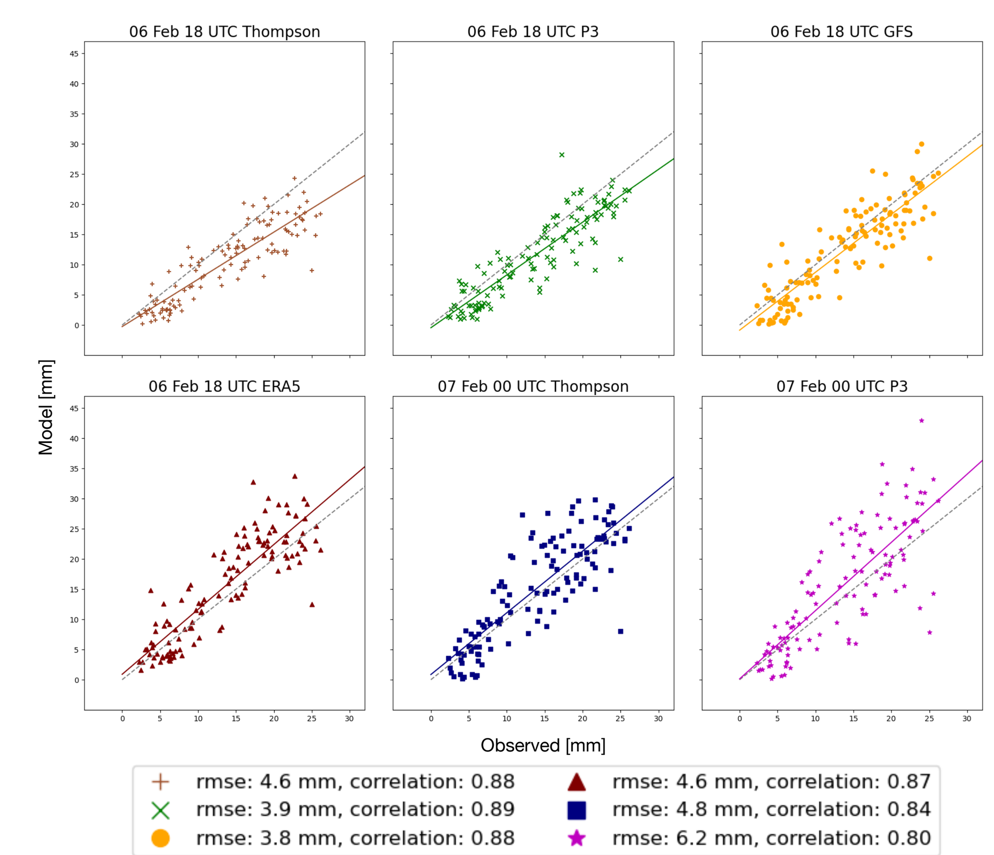

Fig. 9: NY Mesonet/WRF Accumulated Precipitation (12-18 UTC) Scatterplots; the dashed line represents the 1:1 correspondence; the solid line represents the linear regression between the mesonet and the model

- RAP initializations generally under-predict precipitation
  - Thompson scheme produces the lowest values
  - P3 scheme has a low RMS error but still under-predicts in the higher precipitation thresholds
  - All 00 UTC (7 Feb) initializations produce higher precipitation amounts
  - Consistent with the different amounts of riming within each simulation
- GFS initialization has a slightly lower RMS error during this period
- ERA-5 initialization has a similar distribution to the GFS initialization
- Part of the under-prediction is also a displacement error in WRF, with a sharp cutoff east of the frontal zone

6. Conclusions/Future Work

- The lack of a concentrated region of frontogenesis along the deformation axis, along with the lack of a strong 700 hPa low, contributed to the lack of a well-defined primary snowband
- The large regions of low stability or potential instability, a high degree of riming, and aggregation closer to the surface contributed to the high precipitation rates within the region
- WRF generally captures the thermodynamic structure and precipitation field, but simulations with lower degrees of riming (such as the Thompson scheme) under-predict total precipitation
- Future work:
  - Determine the phase space of the different types and scales of snowbands, extending beyond Ganetis et al. (2018)
  - Categorize this event within the new phase space of snowbands

Acknowledgements: This work was supported by NASA Grants 80NSSC19K0394 (SBU) and 80NSSC19K0338 (UW). Thanks to the IMPACTS team for collecting the data, and Laura Tomkins (NCState) for providing the NEXRAD post-processing.